NREL
NATIONAL RENEWABLE ENERGY LABORATORY

Evaluation of Maxim Module-Integrated Electronics at the DOE Regional Test Centers

Preprint

Chris Deline and Bill Sekulic
National Renewable Energy Laboratory

Josh Stein
Sandia National Laboratories

Stephen Barkaszi
Florida Solar Energy Center

Jeff Yang and Seth Kahn
Maxim Integrated

Presented at the 40th IEEE Photovoltaic Specialists Conference (PVSC-40)
Denver, Colorado
June 8-13, 2014

NREL is a national laboratory of the U.S. Department of Energy
Office of Energy Efficiency & Renewable Energy
Operated by the Alliance for Sustainable Energy, LLC

This report is available at no cost from the National Renewable Energy Laboratory (NREL) at www.nrel.gov/publications.

Conference Paper
NREL/CP-5J00-62024
July 2014

Contract No. DE-AC36-08GO28308

NOTICE

This report is available at no cost from the National Renewable Energy Laboratory (NREL) at www.nrel.gov/publications.

Available electronically at http://www.osti.gov/scitech

Available for a processing fee to U.S. Department of Energy and its contractors, in paper, from:

U.S. Department of Energy
Office of Scientific and Technical Information
P.O. Box 62
Oak Ridge, TN 37831-0062
phone: 865.576.8401
fax: 865.576.5728
email: mailto:reports@adonis.osti.gov

Available for sale to the public, in paper, from:

U.S. Department of Commerce
National Technical Information Service
5285 Port Royal Road
Springfield, VA 22161
phone: 800.553.6847
fax: 703.605.6900
email: orders@ntis.fedworld.gov
online ordering: http://www.ntis.gov/help/ordermethods.aspx

Cover Photos: (left to right) photo by Pat Corkery, NREL 16416, photo from SunEdison, NREL 17423, photo by Pat Corkery, NREL 16560, photo by Dennis Schroeder, NREL 17613, photo by Dean Armstrong, NREL 17436, photo by Pat Corkery, NREL 17721.

Evaluation of Maxim Module-Integrated Electronics at the DOE Regional Test Centers

Chris Deline,[1] Bill Sekulic,[1] Josh Stein,[2] Stephen Barkaszi,[3] Jeff Yang,[4] Seth Kahn[4]

[1]National Renewable Energy Laboratory, Golden, CO, 80401, USA

[2] Sandia National Laboratories, Albuquerque, NM, 87123, USA

[3]Florida Solar Energy Center, Cocoa, FL, 32922, USA

[4]Maxim Integrated, San Jose, CA 95134, USA

***Abstract* — Module-embedded power electronics developed by Maxim Integrated are under evaluation through a partnership with the Department of Energy's Regional Test Center (RTC) program. Field deployments of both conventional modules and electronics-enhanced modules are designed to quantify the performance advantage of Maxim's products under different amounts of interrow shading, and their ability to be deployed at a greater ground-coverage ratio than conventional modules. Simulations in PVSYST have quantified the predicted performance difference between conventional modules and Maxim's modules from interrow shading.**

Initial performance results have identified diffuse irradiance losses at tighter row spacing for both the Maxim and conventional modules. Comparisons with published models show good agreement with models predicting the greatest diffuse irradiance losses. At tighter row spacing, all of the strings equipped with embedded power electronics outperformed their conventional peers. An even greater performance advantage is predicted to occur in the winter months when the amount of interrow shading mismatch is at a maximum.

***Index Terms* — partial shading, MLPE, embedded power electronics, PV system performance, diffuse view factor**

I. Introduction

The U.S. Department of Energy (DOE) seeks opportunities to increase U.S. manufacturing and deployment of photovoltaics (PV). A key barrier to the success of new PV technologies is demonstrating the performance and reliability at a level that gives investors adequate confidence for large-scale investments. The DOE created the Regional Test Centers (RTCs) to help companies bridge this "valley of death" by providing infrastructure to rapidly test new products. The RTCs include field installations and performance-monitoring infrastructure in five states (CO, NM, FL, VT, and NV), along with collaborations with multiple commercial partners.

Maxim is one such RTC partner, with evaluation systems currently installed in Colorado and under construction in New Mexico and Florida. Maxim Integrated is a manufacturer of power electronics chips and modules, including a line of PV module-embedded power electronics. The VT8012 and VT8020 printed-circuit assembly (PCA) is designed for direct integration within the PV laminate to improve energy delivery under mismatch conditions.

Maximum energy delivery for a traditional PV system suffers when there is any source of power mismatch between PV cells, such as: manufacturing tolerance mismatch, temperature gradients, nonuniform shadowing, soiling, and cell aging [1-4]. Using a high-efficiency DC-DC converter and fast MPPT algorithm, the VT8012 PCAs reduce energy losses resulting from mismatch within and between PV modules.

Interrow shading can be one source of mismatch in a PV system, and can occur particularly in PV installations with a high Ground-Cover Ratio (GCR). GCR is variously defined as the ratio of module area to total land area, or, neglecting the unshaded first-row: $GCR = L/R$, where L is the length along the array and R is the row-to-row pitch (Fig. 1). The tighter the row-to-row pitch, the larger the GCR.

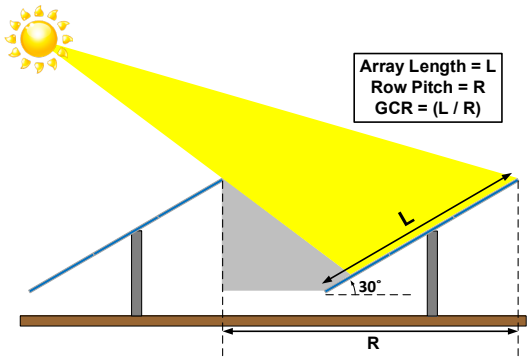

Fig. 1: Interrow shading can be calculated as a function of the GCR, defined as the ratio of PV module area to land area, or simply as the ratio of the array length L to the row pitch R.

When choosing an array row pitch, a trade-off exists between increased energy production per land area (kWh/m^2), and reduced production per rated kiloWatt (kWh/kW) owing to interrow shading losses. This trade-off has been investigated before in several instances of fixed-tilt [5,6] and tracking [6-8] PV systems. By including embedded power electronics, partial shading losses can be reduced, which in turn makes higher power-density installations more

Fig. 2: Maxim VT8012 chipset embedded in the PV laminate. This "smart module" includes submodule power conversion in place of backplane diodes. Six of these DC-DC converters are integrated into each VT8012 PV module.

economical. Detailed performance and economic models such as PVSYST [9] and SAM [10] can be employed to estimate the impacts of different row spacing, and the use of embedded electronics. It is the intent of this work to help experimentally validate such models.

II. Description of Maxim Embedded Electronics

Other commercial module-level power electronics (MLPE) provide power conversion at the module level, with products either mounted to the module frame or installed in the PV junction box [11]. By contrast, Maxim's VT8012 and VT8020 chips are embedded directly into the PV laminate, and distributed every 12–24 cells, for a total of 3–6 per module in place of conventional bypass diodes (Fig. 2). Integration with the PV laminate is done directly on a conventional PV manufacturing line, greatly reducing the cost associated with MLPE by reducing packaging and cabling costs.

VT8012 chips employ a buck DC-DC converter to match the currents of lower-producing solar cells to the current of the remaining cells in the series string. The converter boasts a CEC efficiency of 98.7% and small footprint (< 350 mm^2), as well as compatibility with standard flash IV curve measurement methods.

The performance benefits of these distributed electronics accrue by enabling different portions of the PV module to operate at different peak operating currents. Conventionally, partial shading on one portion of a module would result in one of two behaviors. The bypass diode can short out the shaded submodule, preventing that section from contributing any power to the series total. Alternatively, the entire module and series string might be operated at the reduced power level of the shaded submodule. When equipped with distributed electronics, subsections of the PV module are able to operate independently from each other, with each portion of the module peak power tracked individually, and contributing to the system total (Fig. 3).

Maxim Solar Cell Optimizers perform maximum power-point tracking (MPPT) on each cell string within the PV module. The Optimizer replaces the bypass diode, providing both protection and MPPT functions from one device.

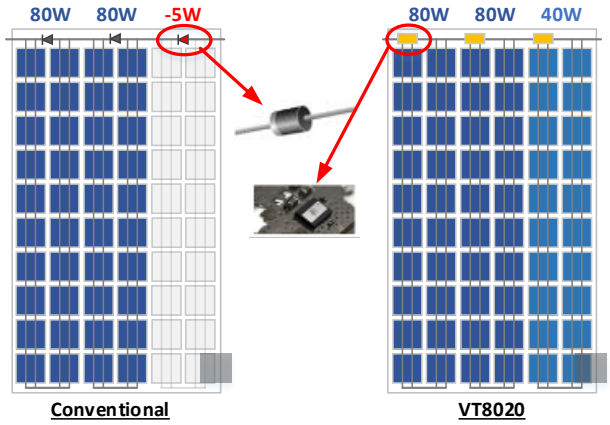

Fig. 3: Comparison of effect of partial module shading. In the conventional case, bypass diodes short out shaded submodules to match current in the rest of the string. With power electronics, shading loss is reduced.

All MLPE systems can offer the ability to mitigate the impact of module-to-module mismatch mechanisms, such as: factory binning tolerances, field degradation, and mismatch from soiling, and near-object shading. However, the submodule optimization offered by Maxim significantly improves performance in cases where the loss mechanism is not spread uniformly across the panel itself. In these examples, not only does each panel perform to its maximum potential but each cell-string within the panel does, as well.

One common and powerful example is the ability to mitigate row-to-row shading losses in fixed-tilt arrays. Row spacing is typically chosen to limit losses from interrow shading. Isolating and optimizing each cell string within the panel offers a significant opportunity to improve production by increasing array density; enabling a PV system to be designed with a more economical trade-off between seasonal shading exposures and higher installation densities.

Figure 4 shows a typical shade derating plot, illustrating how energy production decreases as ground coverage is increased. Panels enabled with Maxim's VT8012 afford the ability to design the array at much higher ground-coverage ratio while producing the same kWh/kWp performance rating.

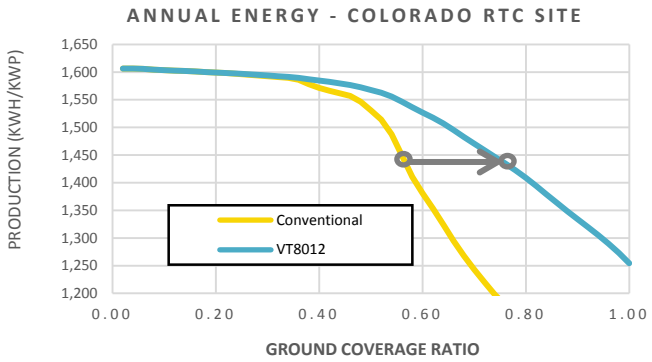

Fig.4: Modeled shade derating with conventional versus Maxim embedded PV modules conducted for the CO RTC site described below. Model results follow methodology of Section III.

As indicated by the gray arrow, panels with embedded Maxim electronics can enable the same energy production per panel at higher ground-coverage ratios and tighter row pitches. An area-constrained roof or ground site can be packed at a higher density to provide more energy at an equivalent or lower levelized cost of electricity (LCOE).

III. Performance Modeling Methodology

Performance modeling of cell-string level optimization is possible using the PVSYST performance modeling software. The software tool provides sufficient flexibility to model the ground coverage density benefits achieved with Maxim's embedded power electronics.

Considerations for modeling cell-string level optimization are similar to those made when modeling different solar panel racking and wiring configurations. For example, when conventional panels are mounted in a stacked-racking configuration, the DC wiring is typically strung horizontally across the racks so that the series of panels closest to the ground are not electrically in series with panels higher off the ground. With this configuration, shown in Fig. 5, an interrow shadow impairs only the bottommost row of panels while the more elevated panels remain at full production.

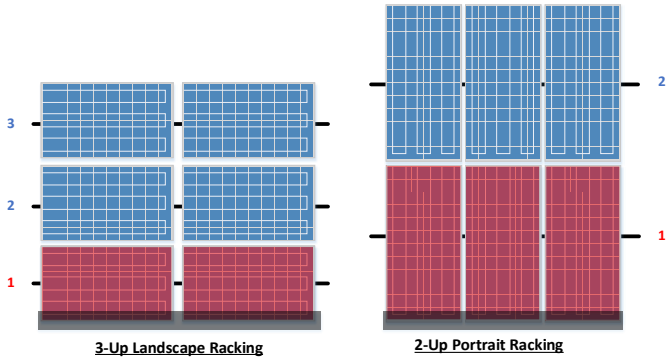

Fig. 5: Electrical regions and shadow susceptibility of conventional panels

PVSYST simulations account for these designs with appropriate selection of the "# of electrical regions" parameter: 3 for the landscape example, and 2 for the portrait example in Figure 5.

As shown in Fig. 6, the Maxim chips offer improved shade tolerance due to the granularity of electrical isolation and degree to which PV performance is maintained under partial shading conditions.

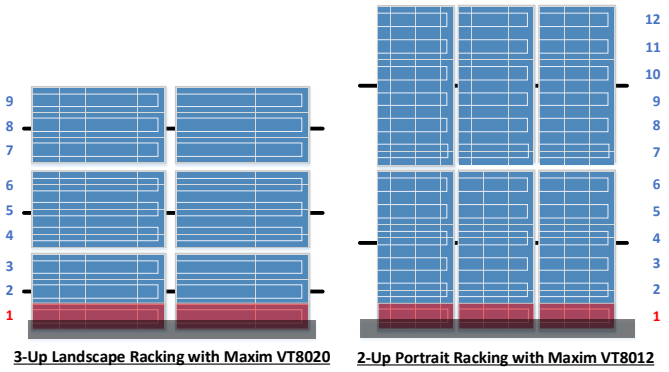

Fig. 6: Electrical regions and shadow susceptibility of VT80XX panels

PVSYST simulations can properly account for the cell-string level optimization, again with an appropriate selection of "# of electrical regions" parameter. This parameter should be set to 9 for the VT8020 landscape example and to 12 for the VT8012 portrait examples above.

IV. Evaluation Installation

The 40-kW field evaluation described here is intended to investigate the energy produced under four different row-spacing conditions. With rows spaced closer together, losses from interrow shading and diffuse field-of-view blocking increase. The ability of VT8012 chips to recover lost performance at closer row spacing will be evaluated over a multiple-year performance assessment.

Evaluation installations are under construction at three of the RTC sites, in CO, NM, and FL. This initial publication is focused on the Colorado installation, completed in April 2014 (Fig. 7). Valid side-by-side comparisons are enabled by including conventional PV modules in rows along with the Maxim product. To ensure a fair comparison, the conventional modules and Maxim modules are sourced from the same manufacturer, using a similar bill-of-materials.

Fig. 7: Maxim installation at the Colorado RTC site

The layout of the Maxim demonstration site is designed to enable two comparisons. The first is the performance of Maxim modules against conventional panels for the same interrow spacing; this is possible because several rows contain strings of Maxim panels and strings of conventional panels.

The second comparison is the performance of different row spacings against the unshaded first row. Because the first row contains both a conventional string and a Maxim string, subsequent close-packed rows can be compared with the performance of the associated first-row string.

Figure 8 shows a layout of the different modules within the Maxim installation. The installation consists of five rows of 72-cell panels in 1-up portrait configuration with a 30-degree tilt angle. Three separate GCR values are chosen to define the system interrow spacing.

Panels are deployed in strings of 10, with each string individually peak-power tracked. To limit "edge effects" where early-morning shade can be cast at an angle to the rows, the outermost three modules in each row are included in separate strings. These "dummy" strings are not considered in this analysis.

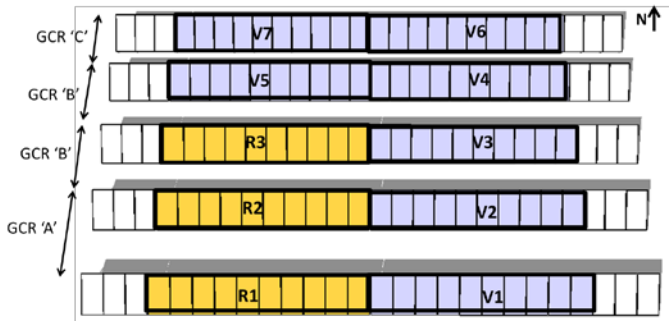

Fig. 8: Layout of the Maxim installation at 3 RTC sites. Strings are indicated by the bold line boxes. Yellow R1 – R3 strings are conventional "reference" modules without power electronics. Blue V1 – V7 strings are Maxim VT8012 modules. Row spacing decreases toward the back of the installation to increase shading loss. Unmarked panels at the edge are "dummy" shading panels.

Each string of 9–10 panels is indicated by R1–R3 for the conventional "reference" modules without electronics, and V1-V7 for the Maxim VT8012 modules. Rows 1–3 include both Maxim and reference modules for side-by-side comparison (V1 vs R1, V2 vs R2, etc.). Rows 4 and 5 were designed to only include Maxim modules. Successively smaller interrow spacing is used to increase the amount of interrow shading on each row. This will allow the performance of the VT8012 modules to be judged at different row spacing.

Per string peak-power tracking is accomplished by seven Power-One PVI-6000 dual-channel inverters. 1-minute sample DC string measurements are provided by the inverter, as well. Comparison with isolated voltage transducers on four of the strings found the integrated inverter DC power measurements to be within 1% under steady-state irradiance conditions (< 10 W/m^2 change in 1 minute) and for irradiance > 200 W/m^2. Plane-of-array irradiance is monitored with a thermopile pyranometer as well as with calibrated reference modules.

To account for any initial offset in performance due to variations in module power ratings, outdoor performance data are adjusted by factory flash-simulator data collected at standard test conditions.

V. Initial Performance Results

A. Modeled Results

The simulations of partial shading response provide the estimates of annual performance losses shown in Table 1. The GCR value provided here is specific for the Colorado installation.

TABLE 1: ESTIMATED SHADING LOSSES FOR DIFFERENT ROW SPACING

	GCR 'A'	GCR 'B'	GCR 'C'
Ground Coverage Ratio	0.45	0.53	0.63
Row Pitch	4.4m	3.7m	3.1m
Conventional Loss	2.9%	6.5%	17%
VT8012 Loss	1.8%	2.9%	5.9%
VT8012 Improvement	1.2%	3.8%	13%

As can be seen in the monthly production chart of Fig. 9, most gains from row-to-row shading are realized in the winter months. The case with ground-coverage ratio 0.53 is simulated to have gains as high as 38% in the month of December.

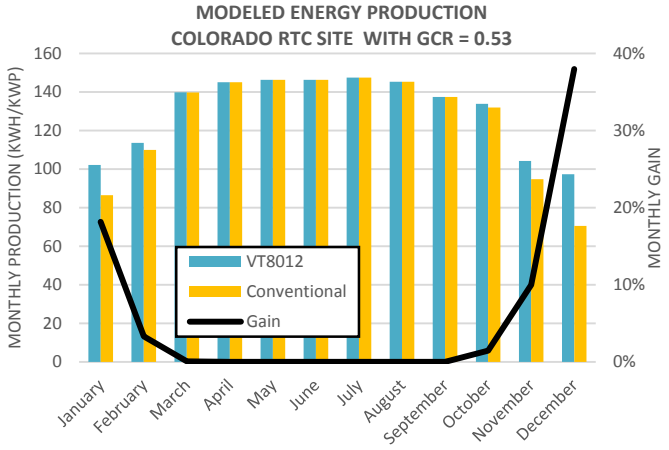

Fig. 9: PVYST simulation results indicating expected monthly performance gains of Maxim versus conventional panels in the Colorado RTC site at the fixed ground-coverage ratio of 0.53.

B. Experimental Results

From simulations above (Fig 9), we can see that the majority of the predicted shading loss in the system occurs in the winter months from October–March. However, this evaluation installation was not completed until April 2014, which means that the performance data collected so far does not account for the most extensive shading conditions that this system will encounter. One type of partial shade mismatch that can be evaluated now is how diffuse irradiance is reduced at different row spacing.

Models for the effect of different row spacing on diffuse and reflected components of irradiance can be found in [12,13]. The reduction in diffuse irradiance is calculated through a "screening angle" $\psi(z)$, which indicates the angle at which the view of the sky is reduced from a given point on the array. Geometry suggests that reduced row spacing increases the screening angle, and decreases the amount of diffuse and reflected irradiance available to the solar module. Interestingly, the same equations can provide different shade-loss predictions, depending on the height z along the PV module that is taken to calculate ψ. For instance, the bottom of the module $z = 0$ receives less diffuse irradiance than the very top. This is illustrated in Fig. 10 for a module at 30° tilt at three different row pitches. It is clear that the bottom half of the module receives considerably less diffuse irradiance than the top half. It is therefore also clear that the calculated performance loss for the system depends on what point along the module is chosen to calculate the shading loss for the system.

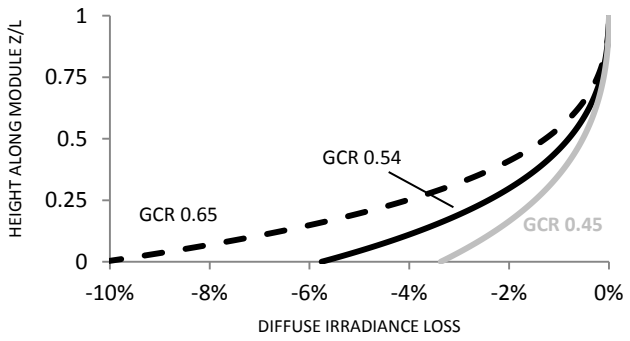

Fig. 10: Diffuse irradiance loss along a PV module (tilt = 30°) at three different ground-coverage ratios [12].

The authors in [14] suggest that PV performance is best modeled by assuming that module current is limited by the lowest irradiance; therefore $z = 0$ should be used to calculate reduced diffuse irradiance. The authors in [12] suggest that averaging $\psi(z)$ over all z is the most appropriate, resulting in a less strict diffuse loss term. This ambiguity can be resolved by comparing different model assumptions with the experimental results.

Figure 11 shows diffuse irradiance loss, predicted by the diffuse screening angle of [12] and the reduced ground-reflected model of [13] at different ground-coverage ratios. Three different $\psi(z)$ values are assumed, one by averaging over all z, one assuming a worst-case screening angle at $z = 0$, and an in-between case taken 10% up the module ($z = L/10$). Ground albedo is assumed to be $\rho = 0.2$ for all cases.

The measured performance of 10 different strings (V1–V7 and R1–R3) is then compared under overcast conditions. The first row of each module type (V1 or R1) is used as the reference against which each other row is compared. Data are collected for three weeks, and selected for high diffuse irradiance conditions ($E_{Diff}/E_{POA} > 0.8$) and $E_{POA} > 200$ W/m^2.

Beam irradiance is further factored out of results by subtracting the estimated contribution of beam irradiance from each string's power:

$$P_{beam} \approx P_{V1}\left(\frac{E_{beam}\cos(\alpha_{AOI})}{E_{POA}}\right)$$

where P_{V1} is the power of string V1, E_{beam} and E_{POA} are the direct-normal and total plane-of-array components of irradiance, respectively, and α_{AOI} is the solar incidence angle to the tilted module plane. The diffuse loss of strings V2–V7 are then calculated relative to the first row:

$$\text{Diffuse Loss} = \frac{P_{VX} - P_{beam}}{P_{V1} - P_{beam}} - 1$$

where P_{VX} is the power of string V2–V7. A similar method is used to determine the diffuse loss of strings R2 and R3, relative to the front-row R1. Figure 11 shows these values, averaged over the three-week period of performance.

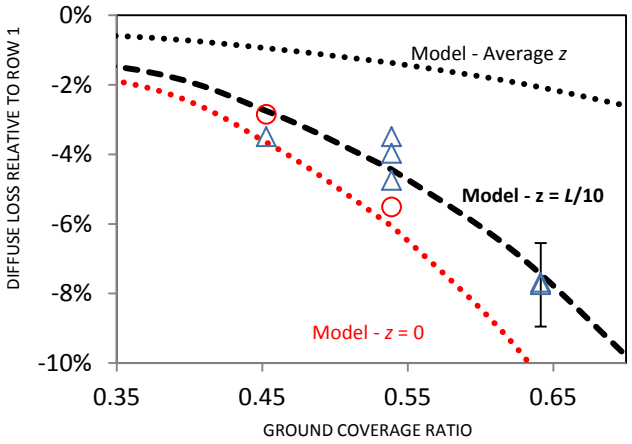

Fig. 11: Diffuse irradiance loss at three different ground-coverage ratios. Modeled results from [12,13] with three diffuse screening angles $\psi(z)$ assumed—averaged across the entire module (average z), at the bottom of the module ($z = 0$), and 10% up the module's length ($z = L/10$). Experimental VT8012 (triangle) and conventional (circle) results displayed similar behavior, with VT8012 strings outperforming the conventional string at larger GCR. Measurement error bars are representative for all experimental data.

The experimental results suggest that the modeled case of $z = 0$ and particularly $z = L/10$ fit the experimental results much more closely than the optimistic average z model. This can be explained from an electrical standpoint by noting that for conventional series-strung PV cells, the module current is limited mainly by the lowest-producing cell within that module. This is less strictly the case for modules with embedded electronics in them.

Comparing conventional with VT8012 results is difficult because no conventional strings were deployed at the tightest row pitch. Although all VT8012 strings slightly out-performed the conventional string at the middle GCR value, the performance of the conventional and VT8012 strings were more equivalent (within measurement uncertainty) at the

broadest row spacing. Although additional comparisons at GCR = 0.65 would confirm this trend, it is possible that the VT8012 strings are outperforming conventional strings at the middle GCR value because the irradiance mismatch is greater. With a 6% diffuse loss at GCR = 0.54 and only 3% loss at GCR = 0.45, there is more opportunity for the losses to be recovered by VT8012 modules at the tighter row pitch. At GCR = 0.45, the relatively low mismatch may be too small for the Maxim DC-DC converter to provide much benefit.

It should be noted that the diffuse irradiance losses investigated here are only a portion of the expected losses from interrow shading in this system. The energy lost from beam shading is expected to be a larger contributor to annual system performance, but this shading occurs only in the winter months. A full year of performance monitoring is required to get a complete picture of the partial shading benefits of Maxim's VT8012 modules.

Conclusion

Theoretical and experimental results are presented for a system employing module-embedded power electronics. PVSYST modeling of the system suggests that partial-shading losses are concentrated in the winter months, and that tighter row spacing can be used with Maxim VT8012 modules to achieve the same annual performance.

A comparison of performance at different row spacing suggests that diffuse-irradiance losses are greater than some models predict. At tighter row spacing, the VT8012 strings all outperformed the conventional string, indicating that a performance advantage is conferred even under diffuse-irradiance mismatch gradients as low as 6%. Performance data during the most-shaded times of the year have not yet been collected, which would enable a full evaluation of these modules' partial-shading benefits.

Acknowledgement

This work was supported by the U.S. Department of Energy under Contract No. DE-AC36-08-GO28308 with the National Renewable Energy Laboratory.

References

[1] S. MacAlpine, M. Brandemuehl, and R. Erickson. "Characterization of Power Optimizer Potential to Increase Energy Capture in Photovoltaic Systems Operating Under Nonuniform Conditions," IEEE Transactions on Power Electronics **28**, pp. 2936-2945, 2013.

[2] C. Deline, B. Marion, J. Granata, and S. Gonzalez. *A Performance and Economic Analysis of Distributed Power Electronics in Photovoltaic Systems*. NREL Report No. TP-5200-50003. Golden, CO: National Renewable Energy Laboratory, December 2010.

[3] S. MacAlpine, C. Deline, R. Erickson, and M. Brandemuehl, "Module Mismatch Loss and Recoverable Power in Unshaded PV Installations," 38th IEEE Photovoltaic Specialists Conference, 2012.

[4] D. Jordan, J. Wohlgemuth, and S. Kurtz, "Technology and Climate Trends in PV Module Degradation," in 27th European Photovoltaic Solar Energy Conference and Exhibition, PVSEC, Frankfurt, Germany, 2012.

[5] J. Bany and J. Appelbaum, "The Effect of Shading on the Design of a Field of Solar Collectors," Solar Cells **20** pp. 201-228, 1987.

[6] J. Gordon, H. Wenger, "Central-Station Solar Photovoltaic Systems: Field Layout, Tracker, and Array Geometry Sensitivity Studies," Solar Energy **46** pp. 211-217, 1991.

[7] J. Monedero, F. Dobon, A. Lugo, P. Valera, R. Osuna, L. Acosta, and G.N. Marichal, "Minimizing Energy Shadow Losses for Large PV Plants," 3rd IEEE World Conference on Photovoltaic Energy Conversion, 2003.

[8] L. Navarte and E. Lorenzo, "Tracking and Ground Cover Ratio," Progress in Photovoltaics **16** pp. 703-714, 2008.

[9] Mermoud, A., "Use and Validation of PVSYST, a User-Friendly Software for PV-System Design," 13th European Photovoltaic Solar Energy Conference, Nice, France, 736–739, 1995. See also http://www.pvsyst.com/

[10] N. Blair, M. Mehos, C. Christensen, and C. Cameron, "Modeling Photovoltaic and Concentrating Solar Power Trough Performance, Cost, and Financing with the Solar Advisor Model," Proceedings of SOLAR 2008 - American Solar Energy Society, San Diego, California, 2008. See also https://sam.nrel.gov/

[11] C. Deline and S. MacAlpine, "Use Conditions and Efficiency Measurements of DC Power Optimizers for Photovoltaic Systems," IEEE Energy Conversion Congress and Expo (ECCE) 2013, DOI 10.1109/ECCE.2013.6647346

[12] D. Passias and B. Kallback, "Shading Effects in Rows of Solar Cell Panels," Solar Cells **11** pp.281-291, 1983.

[13] D. Goswami, E. Stefanakos, A. Hassan, "Effect of Row-to-Row Shading on the Output of Flat-Plate South-Facing Photovoltaic Arrays," Transactions of the ASME Journal of Solar Energy Engineering **111** (3) pp. 257-259, 1989.

[14] M. Van Schalkwijk, A.J. Kil, T.c.J. Van der Weiden, "Dependence of Diffuse Light Blocking on the Ground Cover Ratio for Stationary PV Arrays," Solar Energy **61** 1, pp. 381-387, 1991.